Communications Earth & Environment https://doi.org/10.1038/s43247-026-03404-3

Article in Press

Global warming increases ammonia emissions and reduces the efficacy of mitigation actions

Received: 24 November 2025

Accepted: 5 March 2026

Cite this article as: Jiang, J., Stevenson, D.S., Uwizeye, A. *et al.* Global warming increases ammonia emissions and reduces the efficacy of mitigation actions. *Commun Earth Environ* (2026). https://doi.org/10.1038/s43247-026-03404-3

Jize Jiang, David S. Stevenson, Aimable Uwizeye, Flavia A. M. Casu, Giuseppe Tempio, Alessandra Falcucci & Mark A. Sutton

Global warming increases ammonia emissions and reduces the efficacy of mitigation actions

Authors: Jize Jiang[1,2,3,*], David S. Stevenson[1,*], Aimable Uwizeye[4], Flavia Casu[4], Giuseppe Tempio[4], Alessandra Falcucci[4] and Mark A. Sutton[5,*]

[1] School of GeoSciences, The University of Edinburgh, Edinburgh, United Kingdom

[2] Department of Environmental Systems Science, ETH Zurich, Zurich, Switzerland

[3] Eawag, Swiss Federal Institute of Aquatic Science and Technology, Dübendorf, Switzerland

[4] Animal Production and Health Division, Food and Agriculture Organization of the United Nations, Rome, Italy

[5] UK Centre for Ecology and Hydrology, Edinburgh, Edinburgh Research Station, Bush Estate, Penicuik, United Kingdom

*Corresponding authors: Jize Jiang (jize.jiang@usys.ethz.ch), David. S. Stevenson (david.s.stevenson@ed.ac.uk), Mark A. Sutton (ms@ceh.ac.uk)

Abstract

Agricultural ammonia (NH_3) emissions adversely affect air quality, threatening ecosystems and human health. The extent to which global NH_3 emissions respond to a warmer climate and the effects of changing agricultural management practices remain poorly quantified. Here, we show that global warming drives NH_3 emission increases of 5-22% across plausible ranges of climate projections in 2091-2100, with >10% regional increase in NH_3 emissions per °C warming. A package of six linked measures could reduce present global agricultural NH_3 emissions by 31% but only by 16-28% globally for contrasting climate scenarios (2091-2100), with up to 97% decrease in the effectiveness of measures at a continental scale. Our study underscores the need to consider temperature dependence when evaluating the efficacy of NH_3 emissions reduction policies under a changing climate, and highlights that achieving ambitious NH_3 emission abatement targets will require enhanced efforts to mitigate climate change.

Introduction

Agricultural intensification in many parts of the world has substantially increased emissions of ammonia (NH_3) to the atmosphere[1,2], the release of which reduces visibility and air quality through formation of secondary particulate matter[3–7], posing risks to human health[8,9]. Once deposited, NH_3 can harm sensitive plant species, including through its alkaline effect, contributing to a loss of biodiversity[10,11]. At the same time, NH_3 volatilization represents a waste of valuable reactive nitrogen (N_r) resources in agriculture[2]. Reducing NH_3 emissions can therefore benefit both the environment and agricultural sustainability.

The dominant source of NH_3 emission is from agriculture[12], often accounting for over 85% of the total NH_3 emissions[3,13]. Non-agricultural sources of NH_3 emissions are much smaller, typically accounting for only 5 to 15% of the total emissions, depending on the region[14]. These sources include biomass burning, transport, industry, residential and some natural sources, such as soil and ocean emissions. Volatilization of NH_3 is strongly dependent on environmental conditions. For example, based on simple thermodynamics, NH_3 volatilization roughly doubles every 5 °C[14]. Accordingly, it has been reported that measured NH_3 emissions from seabird colonies increased about 3 times for an increase of 10 °C (equivalent to $Q_{10} \sim 3$; Q_{10} represents a relative increase in NH_3 emissions for every 10 ºC rise in temperature)[15]. However, agricultural systems are far more complex, so a generalised function that describes the temperature effect on NH_3 volatilization is likely to be over-simplified for human-managed systems; the temperature sensitivity is also constrained by N-pool limitations and alternative fates of ammonium, that depend upon agricultural management decisions.

A widely applied approach for estimating NH_3 emissions is the use of emission factors (EFs), which represent a unit emission rate scaled by activity statistics (such as livestock numbers or fertilizer usage). As EFs can only consider the climatic effects in a limited way, this

approach is unable to provide an accurate representation of the spatial and temporal variations in emissions as climate varies from year-to-year and evolves in the longer term[14]. An alternative approach is the use of process-based models, which are developed based on the theoretical understanding of relevant processes that govern NH_3 emissions[16–24]. Such process-based models can be applied to integrate the main effects of environmental drivers and influences of human activities when calculating NH_3 emissions[21,22,25–28]. For global agricultural NH_3 emissions in the 21st century, two representative process-based models quantified emissions at 35 Tg N yr^{-1} (CAMEO)[29] and 48 Tg N yr^{-1} (FANv2)[27], while estimates based on EFs[30–33] reported varying emissions from 32 to 54 Tg N yr^{-1}.

Global agricultural NH_3 emissions have increased sharply since 1970[33], largely due to intensified crop and livestock production[34]. Meanwhile, warming further enhances NH_3 volatilization, making climate change an increasingly important driver of future emissions. A recent study estimated that global NH_3 emissions from three major crop production systems are projected to increase by 5-16%[35] following different climate trajectories. Under scenarios of intense warming, emissions could increase by up to 40% in central to northern Europe[36], by 81% in the US cropland[37] and by 32% in China's cereal production systems[38]. While these studies provide valuable insights into the climate-driven NH_3 emissions from croplands, they largely omit livestock systems, which account for a substantial share of global agricultural NH_3. More-comprehensive assessment, including both crop and livestock systems, has suggested that global emissions may increase by 42% due to a 5 ºC temperature rise[14], or by 7%-22% under alternative climate projections[29]. The wide range of estimates arising from different empirical and modelling approaches highlights persistent uncertainties in quantifying climate-dependent NH_3 emissions, and highlights the need to evaluate the effectiveness of mitigation actions in a warming climate.

In this study, we address these gaps using AMCLIM[23,24], a recently developed process-based emission model that explicitly quantifies agricultural NH_3 emissions in relation to N_r flows in both crop and livestock systems. AMCLIM integrates the effects of environmental factors on N processes and accounts for major sectoral differences in management practices (see Methods). Our simulations show how NH_3 emission is co-determined by environmental factors and management practices (Fig. 1 and Supplementary Fig. 1), and how temperature sensitivity of NH_3 volatilization varies strongly across climatic conditions and agricultural activities. We further make projections of warming-driven NH_3 emissions for the mid-term (2041-2050) and long-term (2091-2100) under several climate scenarios, and assess how global warming alters the effectiveness of mitigation measures. Our findings show how projected warming can substantially reduce the efficacy of NH_3 abatement measures, which have important implications for future air quality and N management.

Global agricultural NH_3 emissions

Through application of AMCLIM, we estimate global agricultural NH_3 emissions at 44.9 Tg N yr^{-1} in 2010, which is comparable to other studies[27,28,33] (see Supplementary Note 2 and Supplementary Table 1). Taking account of climatic and management differences, our simulations show the highest agricultural emissions of NH_3 to occur in South Asia, East Asia, Europe, North America and South America (Fig. 1a). To illustrate the consequences of climatic and management differences on emission patterns, we applied the AMCLIM results to establish globally averaged EFs, which were then mapped using activity statistics (Methods). Figure 1b, shows that regional emissions based on the full AMCLIM modelling can be 50% larger or 40-60% smaller than the simple EF approach, highlighting the importance of incorporating spatial variability in climate and management practices. This comparison reveals that the use of simple EF estimates for NH_3 would substantially overestimate emissions in many northern and other

cooler regions and underestimate emissions in hotter and more continental locations. The pattern shown in Fig. 1b is complex, reflecting the combined effects of spatially varying climatic conditions and management practices.

Most NH_3 emissions occur in the northern hemisphere (Figure 1a and Supplementary Fig. 2), with largest emissions in spring and summer (Supplementary Fig. 3). Peak emissions exceeding 50 kg N ha^{-1} yr^{-1} occur in the North China Plain (NCP), northern India, Pakistan and the Netherlands (Fig. 1a); emissions over 20 kg N ha^{-1} yr^{-1} are widespread in the eastern US, India, and parts of Southern America and Europe, with the dominant source of emissions being spatially different (Supplementary Figs. 4-5). We estimate China, India, US, Brazil and Pakistan to be the top five countries contributing to NH_3 emissions at 8.8, 7.4, 4.5, 3.0 and 2.0 Tg N yr^{-1}, respectively, which together account for nearly 60% of global emissions. Our simulations suggest that ~2/3 of emissions result from livestock farming (housing, manure storage/processing systems and manure applied to land), with ~1/3 of NH_3 emissions from the use of synthetic fertilizer (Supplementary Fig. 6). Cattle represent the largest sector share, contributing 60% of livestock emissions and nearly 40% of total agricultural emissions (Supplementary Fig. 6).

Temperature sensitivity of NH_3 emissions

Based on temperature perturbation experiments, we find that a 2 °C rise in temperature results in global annual agricultural NH_3 emissions increasing by 7.0%, while NH_3 emissions decline by 6.4% when temperature is reduced by 2 °C (Table 1). Going beyond this range can give non-linear responses that also differ by emission source (Supplementary Table 2). The largest absolute increase in agricultural NH_3 emissions due to 2°C additional warming occurs at

20°N to 40°N (Supplementary Fig. 7a), and the highest relative increase in NH_3 emissions is found in polar regions north of 60°N (Supplementary Fig. 7b).

Table 1 distinguishes the percentage changes in emissions from the percentage changes in the fraction of available N that is emitted (P_V) at each stage. For most sources, the two values are the same. However, NH_3 emissions from manure storage/processing and application to land depend on previous activities, i.e. earlier stages of the processing of N_r in the system. If higher NH_3 emissions originate from previous stages, less ammoniacal N in livestock excreta is available, resulting in less NH_3 emissions from subsequent activities. As a result of this interaction, while the relative change in P_V for manure application is 6.8%, the total NH_3 emissions from this source only increase by 2.9% with a 2 °C increase (Table 1).

Table 1: Results of temperature perturbation experiments. Percentage changes in global NH_3 emissions and the percentage of available nitrogen volatilized (P_V) due to 2 °C temperature changes.

	ΔNH_3 emission (%)		ΔP_V (%)	
Activity	+2 °C	–2 °C	+2 °C	–2 °C
Synthetic fertilizer	+7.4	–6.7	+7.4	–6.7
Livestock housing	+10.0	–9.5	+10.0	–9.5
Manure storage (inc. manure processing)	+8.7	–8.0	+11.0	–9.7
Manure application to land	+2.9	–0.8	+6.8	–4.7
Grazing	+5.2	–5.4	+5.2	–5.4
Total	+7.0	–6.4	+7.0	–6.4

Globally, we find a temperature sensitivity of NH_3 volatilization that represents 3.4% relative increase in NH_3 volatilization for each 1 °C increase in mean temperature, compared to the baseline results for the year 2010 (with substantial regional differences and differences between emission stage as shown in Fig. 2). We find especially high temperature sensitivity for synthetic fertilizer (Fig. 2a and 2b), with values over 10% $°C^{-1}$. For manure storage (including manure processing), high temperature sensitivity frequently occurs in cold environments such as northern Europe, Siberia and Tibet (Fig. 2d). In regions with hot temperature such as within in the tropics, almost complete volatilization of ammoniacal N (TAN) pools limits further emission with warming, thereby reducing the temperature sensitivity. For intensive livestock housing, the effect of temperature can be smaller due to management of temperature in livestock houses[16,24]. Even though we have accounted for this effect, we still find substantial temperature sensitivity of NH_3 emissions from livestock housing (4.9% $°C^{-1}$), which is particularly seen in areas dominated by more informal livestock housing systems (i.e., partially enclosed and naturally ventilated livestock houses made with local materials like mud bricks or timber) such as in Africa (Fig. 2c).

Overall, the effect of warming on NH_3 emissions estimated in this study (3.4% $°C^{-1}$) is smaller than 8.4% $°C^{-1}$ found by Sutton et al.[14] who applied empirical relationships to estimate the temperature sensitivity. This is especially seen for manure application to land and grazing in Australia, the Middle East and Sahel regions (Fig. 2e and 2f), largely because most ammoniacal N is already lost as NH_3 under current conditions. In hot climates, while the volatilization potential increases substantially, in practice this can be constrained by limitation in the amount of remaining TAN available for volatilization. In extremes, once all TAN is volatilized, additional warming cannot increase emissions further. By contrast, temperature sensitivity tends to be high in regions with low NH_3 volatilization because emission increases substantially when the environment gets warmer, while there is no TAN limitation to further emissions (only a small percent of the available TAN is volatilized). These cases can be particularly seen in places with low P_V values for synthetic fertilizer use (Fig. 2b and Supplementary Fig. 8b).

The temperature dependence in this study is similar to the estimate of 3.0% $°C^{-1}$ by Beaudor et al.[29] using the CAMEO model. The similar response of AMCLIM to CAMEO[29] can be considered fortuitous since their estimate is mainly associated with increased soil ammonium content, while their indoor emissions are indirectly dependent on climate through altering net primary productivity which increased their estimated amounts of livestock feed. By contrast, the AMCLIM response focuses on the direct warming interactions of ammonia volatilization.

On the global scale, the temperature sensitivity of livestock housing (4.9% $ºC^{-1}$) is similar to that of manure storage emissions (5.2% $ºC^{-1}$). These values are both higher than the temperature dependence for synthetic fertilizer application to land (3.5% $ºC^{-1}$), manure application (3.5% $ºC^{-1}$) and grazing emissions (2.7% $ºC^{-1}$) (as shown in Table 2). These differences can be partly explained NH_3 volatilization being the dominant N loss pathway for livestock housing and manure storage, whereas other N processes such as nitrification and plant N uptake also deplete the TAN pool for fertilizer and manure application to land, and

grazing. Since those other N processes are also temperature dependent (see Supplementary Note 5 and Supplementary Fig. 9), this affects the overall temperature dependence of NH_3 volatilization for fertilizer and manure application and grazing. In this way, the difference in temperature dependence between housing/storage and land-application/grazing, give an indication of the extent to which these other field-related factors reduce more direct temperature dependence of NH_3 emissions. These effects are distinct from those that also result from the depletion of TAN through the manure management chain (from housing, to storage, to spreading). As shown in Table 1, the effect of temperature on total NH_3 emissions for manure storage/processing and manure application is smaller than the corresponding effect on P_V. Thus, the differences in P_V reflect the mix of contributing temperature dependent processes, while the differences in total NH_3 emissions also reflect temperature related interactions associated with the depletion of TAN through the manure management chain. The responses are further complicated by interactions with water availability, where sufficient moisture is needed to allow (temperature-dependent) urea hydrolysis as a precondition for NH_3 emission, which can also be reduced in conditions of high rainfall and wet soils due to the high solubility of NH_3 (Fig. 2b).

Implications for future NH_3 mitigation strategies at global and regional scale

Our results highlight the importance of considering NH_3 emission mitigation in an integrated way, especially given the context that climate change is projected to increase emissions[29,35]. All source activities need to be targeted at the same time because of the close link between the sequential stages in agricultural systems[39,40]. Hence mitigating emissions from only housing or storage would increases emissions from manure application, unless measures are taken at all three stages. Conversely, efforts to reduce NH_3 emissions from application of manure are

compromised if a large fraction of N has already been lost due to lack of measures taken to reduce N losses at earlier management stages, with the consequence that manure becomes less valuable as a nitrogen resource.

Practices to reduce agricultural NH_3 emissions include: i) optimizing N application rates to meet crop needs[41,42], ii) better application techniques such as incorporation and deep placement of fertilizers and manure[40,43–45], iii) limiting the emission surfaces in animal houses[40], iv) improving animal feed to decrease N surplus in excreta[40,45], v) covering manure stores[40,45], and vi) storing unmanaged manure[45]. By incorporating such a simple package of these six mitigation measures (see Methods and Supplementary Table 3), we estimate that agricultural NH_3 emissions could be reduced by 31% globally (based a 2010 baseline; Table 2 and Supplementary Fig. 10). These measures are found to be generally effective across the globe, with the largest relative reductions in our simulations for East Asia and Europe (Table 2 and Supplementary Fig. 10).

However, when considering the warming effects on NH_3 emissions in a changing climate, we estimate that the same package of measures would be less effective in achieving emission reductions, thereby making it harder to reach environmental policy goals. To assess this, we used a set of future climate projections based on the Shared Socio-economic Pathways (SSPs), which describe alternative trajectories of socio-economic development and associated greenhouse gas emissions. Specifically, we chose SSP1-2.6 (a sustainability-oriented pathway with low challenges to mitigation and adaptation), SSP2-4.5 (a “middle-of-the-road” pathway with moderate challenges), SSP3-7.0 (a regional rivalry pathway characterized by high population growth, limited technological development, and high challenges to mitigation), and SSP5-8.5 (a fossil-fuel-driven development pathway with high energy demand and very high emissions)[45]. These scenarios span a range of radiative forcings increasing from 2.6 to 8.5 W m^{-2} and were analysed for the mid-century (2041–2050) and late-century (2091–2100) periods.

Assuming the same activity data and management practices as the year 2010 (i.e., using only the **temperature** outputs of these scenarios), we project increases in NH_3 emissions by 4.6±1.4% (SSP1-2.6, where the range represents 1x standard deviation from 8 climate models for 10-year simulations), 9.9±2.5% (SSP2-4.5), 15.2±4.0% (SSP3-7.0) and 21.7±5.3% (SSP5-8.5) in 2091-2100 (Figs. 3-4 and Table 2), as a result of warming. Under an ambitious climate mitigation scenario (SSP1-2.6), we find that global warming has small effects in increasing NH_3 emissions, and the collective package of NH_3 mitigation measures can still largely achieve the anticipated outcome (with globally 90% effectiveness of NH_3 mitigation as the 2010 baseline of no additional warming). By contrast, under SSP5-8.5 (considering a global land temperature increase of 6.5 °C), we find that around half of the mitigation potential (of the measures package without climate warming) is offset by the warming-induced increase in NH_3 emissions. Use of a full set of outputs from these scenarios (including for changed activity statistics) would imply even larger emissions than those which we examine here (see further below).

Based on our analysis, the largest effect of warming is estimated for South America, which is associated with only 0.03 effectiveness of the standard abatement package (i.e., mitigation is almost entirely offset by the warming-induced increase in emissions) compared with mitigation in the absence of climate warming (Fig. 4b). This can be attributed to both a lower mitigation potential of the measures package compared with other regions (Table 2) and a rather high sensitivity to temperature increase (Fig. 4a), which in turn reflects a high share of grazing and fertilizers to total emissions (Supplementary Figs. 4-5).

Our results show that, additional abatement measures would be needed in a warmer climate to achieve the same level of NH_3 emission reduction than achieved in the present climate. It emphasizes the need for substantial action to reduce NH_3 emissions, especially considering that the anthropogenic N_r inputs in the future may increase due to increasing food demand[46], amplifying the tendency to globally increasing NH_3 emissions.

Table 2. Global and regional NH_3 emissions and mitigated emissions in reference year 2010, and projections for 2041-2050 and 2091-2100 using climate data from SSP1-2.6 and SSP5-8.5 (for scenarios, see Fig. 4, with effects of other socio-economic drivers excluded). Bold values in parenthesis are relative reduction compared with the baseline value for the year 2010 in the absence of mitigation.

			SSP1-2.6		SSP5-8.5	
Region		2010	2041-2050	2091-2100	2041-2050	2091-2100
Global	Base	44.9	47.0	47.0	47.9	54.7
	Mitigation	31.1(**31%**)	32.4(**28%**)	32.5(**28%**)	33.2(**26%**)	37.8(**16%**)
Africa	Base	4.4	4.5	4.5	4.6	5.0
	Mitigation	3.3(**24%**)	3.4(**22%**)	3.4(**22%**)	3.4(**21%**)	3.8(**14%**)
N. America	Base	6.2	6.5	6.5	6.7	7.7
	Mitigation	4.3(**31%**)	4.5(**28%**)	4.5(**27%**)	4.6(**26%**)	5.3(**15%**)
S. America	Base	5.2	5.5	5.5	5.7	6.5
	Mitigation	4.1(**21%**)	4.4(**16%**)	4.4(**16%**)	4.5(**14%**)	5.2(**1%**)
E. Asia	Base	9.2	9.6	9.7	9.9	11.4
	Mitigation	5.7(**38%**)	6.0(**35%**)	6.0(**34%**)	6.2(**33%**)	7.1(**23%**)
S. Asia	Base	10.1	10.3	10.4	10.6	12.2
	Mitigation	7.0(**31%**)	7.2(**29%**)	7.2(**29%**)	7.3(**28%**)	8.4(**17%**)
Europe	Base	4.6	4.9	4.9	5.1	5.7
	Mitigation	3.0(**35%**)	3.2(**30%**)	3.2(**30%**)	3.3(**28%**)	3.7(**19%**)
Other	Base	5.2	5.4	5.4	5.5	6.1
	Mitigation	3.7(**29%**)	3.8(**26%**)	3.8(**26%**)	3.9(**25%**)	4.4(**16%**)

High-latitudes are projected to experience more warming than mid- and low-latitudes[47]. Given that the higher temperature sensitivity under cold conditions, there is a substantially greater risk of larger NH_3 emissions increases in high-latitude regions than elsewhere (Fig. 3 and Fig. 4a), with implications for increased pollution, adverse environmental effects and reduced nutrient use efficiency.

We expect that the temperature sensitivity estimated by our approach is probably conservative since we do not include the impacts of higher temperature on soil moisture change. Hence the warming effect could be amplified by further dryness, which can cause more NH_3 emissions under certain circumstances[48–50], given that NH_3 emissions are also regulated by water availability. Similarly, our simulations do not include the effect of leaf-surface interactions on bi-directional NH_3 fluxes, which are expected to increase temperature dependence for field-based emissions[19,23]. Conversely, if a region were to become both hotter and wetter, the

temperature effect could be offset while increasing the share of N_r that is lost as leaching or runoff[23]. We should emphasize that our projections focus specifically on the effect of global warming on NH_3 emissions. The SSP scenarios and variants (e.g. Kanter et al.[51]) also provide outputs related to socio-economic development with corresponding agricultural practices embedded in the SSPs, including dietary change. For example, a SSP scenario that represents substantial future agricultural intensification along with high animal protein intake diets and resource-intensive production would require higher demand of N inputs through fertilizer application and expanded livestock production and further increase NH_3 emissions compared with the effects considered here focusing specifically on temperature. Consideration of such wider socio-economic interactions can be considered as multiplicative to the AMCLIM estimates we present here, and could be explored further in future research. Other drivers that are worth investigating in future research include N the interactions with emission and deposition of nitrogen oxides and changes in land use under contrasting SSPs.

In this study, we highlight the importance of integrating future climate warming into global and regional NH_3 reduction policies. Whereas a simple package of six measures can reduce NH_3 emission substantially, in a warmer world, further and more ambitious measures will be needed to achieve the same level of emission reduction. It is also important to see NH_3 mitigation in the context of actions to “halve the global waste of N_r resources”[52,53]. Based on a typical present fertilizer value of US$1.30 per kg N, the 2010 estimate of global NH_3 emissions represents an annual waste of US$58 billion. Together with other forms of wasted N_r and the wider costs for human health, ecosystems and climate change, it presents a strong case for adopting cost-effective methods to reduce agricultural NH_3 emissions, as part of a wider package of actions towards more efficient management of the N cycle.

Methods

AMCLIM model

We used the AMCLIM version 1.0 model to estimate agricultural NH_3 emissions from livestock farming and synthetic fertilizer use. AMCLIM is a dynamical process-based model that incorporates the effects of environmental drivers on the formation and transport of N compounds to simulate the temporal evolution of various N species, with a focus on NH_3 volatilization. Three modules are specially designed to simulate relevant physical, chemical and biological processes that govern the N flows in agricultural systems while also considering management practices: (a) livestock housing, (b) manure storage (including processing) and (c) application of manure to land. Pools of N compounds are determined by a mass balance approach at every time step, with flows between the N pools calculated. Simulated fluxes depend on the context. Details of simulated physical transport, chemical transformation and plant N uptake are presented in refs[23,24].

Here we focus on describing the volatilization of NH_3, which is a physiochemical process that typically takes place from wet or drying surfaces. Gaseous NH_3 is in dynamic equilibrium with aqueous ammonium depending on the substrate pH and temperature, which can be calculated by the following equations that represent the combined effects of gas solubility (Henry's Law) and aqueous phase dissociation:

$$\chi = \frac{161500}{T}\exp\left(\frac{-10378}{T}\right)\Gamma \quad (1)$$

$$\Gamma = \frac{[NH_4^+]}{[H^+]} = \frac{[TAN]}{K_{NH_4^+} + [H^+]} \quad (2)$$

where K_{NH4+} is the dissociation constant of ammonium (NH_4^+), and Γ is the NH_3 emission potential defined as the ratio of $[NH_4^+]/[H^+]$ in refs[18,54]. TAN is total ammoniacal nitrogen that is an aggregated N species (TAN = NH_3 + NH_4^+).

The concentration difference of NH_3 between the surface and the atmosphere, along with the atmospheric resistances, determine the volatilization of NH_3 (F_{NH_3}, gN m^{-2} s^{-1}) from surface to the atmosphere, which is calculated as:

$$F_{NH_3} = \frac{[NH_3(g)]_{srf} - \chi_{atm}}{R_a + R_b} \quad (3)$$

where $[NH_3(g)]_{srf}$ and χ_{atm} are NH_3 concentrations at the surface and atmospheric NH_3 concentration at a reference height consistent with atmospheric resistances. The atmospheric NH_3 concentration was set to zero in all AMCLIM simulations presented here. R_a and R_b are aerodynamic and boundary layer resistance, respectively. AMCLIM simulates NH_3 volatilization as a uni-directional process, i.e., emission only, and deposition is not simulated. For the sources considered here (fertilizer, manure, urine patches), $[NH_3(g)]_{srf}$ is much larger than χ_{atm} , so that inclusion of χ_{atm} has negligible effect. There is no interaction with surface vegetation, so that surface resistance is excluded in Eq. (3). Therefore, the quantified emissions should be considered as net gross emissions. Conversely, for simulation of bi-directional exchange fluxes with vegetation (not the focus of the present study) the value of χ_{atm} would need to be included[14].

Model input data

There are three major types of geospatial inputs to AMCLIM: meteorological inputs, soil properties and activity data. The AMCLIM model is driven by hourly ERA5 reanalysis meteorology[55], including air temperature, relative humidity (derived from dew point temperature), wind speed, rainfall, soil temperature and water content at two depth levels (0-7, 7-28 cm), and surface and sub-surface runoff fluxes.

Soil properties required by AMCLIM include soil pH, soil texture (sand, clay and silt fraction) and soil organic matter content. These data are from Harmonized World Soil Database (HWSD) v1.2[56].

A wide range of activity data have been extensively used by AMCLIM. For livestock farming, livestock and storage and other manure management systems (MMS) data are obtained from FAO Global Livestock Environmental Assessment Model (GLEAM, https://www.fao.org/gleam/en/). The livestock data contain information on the geographical distribution at a resolution of 1 km x 1 km of livestock population, average live-weight and total N excretion rates, which are categorized by livestock category, species and production system. The global livestock populations and their geospatial distributions were based on FAOSTAT data for 2010 and the Gridded Livestock of the World (GLW) model[57].

For synthetic fertilizer use, the Global Gridded Crop Model Intercomparison Phase 3 (GGCMI3) dataset provides N application data for 16 major crops, including N application rates and total N applied to crops[58,59]. The areas of croplands are then derived from GGCMI3, which have incorporated the harvested area from the Farming the Planet 2 (FTP2) dataset[60].

We use the crop calendars from the GGCMI3 dataset in AMCLIM simulations, which distinguish the planting and harvesting seasons of crops between rain-fed and irrigated systems. The crop calendars are static, based on a climatology, and are used to determine the timing of fertilizer application. The Global Rainfed, Irrigated and Paddy Croplands (GRIPC) dataset is used to classify cropland into rain-fed and irrigated systems and to determine the irrigation events and corresponding crop calendars.

Model simulations

Simulations for livestock farming include the following sectors: cattle (including buffaloes), pigs, chicken, sheep and goats. All three modules in AMCLIM are operated for representing the

activities and different practices of the livestock sectors, from animal housing to manure storage/management and then to the ultimate land application. Ruminant (cattle, sheep and goat) grazing is also specifically modelled to differentiate the processes from land application of fertilizers.

We categorise three N types for synthetic fertilizer use: urea, ammonium and nitrate. Combining the GGCMI3 N application data with IFA country-level synthetic fertilizer consumption statistical data, we split the application rates into fractions of these three groups of applied N. The area of cropland that uses a specific type of fertilizer is proportional to the fraction of the fertilizer used.

The AMCLIM model has been applied at site scale and has been intensively evaluated by a series of detailed comparison of time series between measured and modelled fluxes for agricultural activities[23,24]. Global simulations were conducted for the reference year 2010 on a longitude-latitude grid at a resolution of 0.5° × 0.5° (equivalent to 39 km x 55 km at 45º latitude) and were performed at an hourly time step. All model inputs were resampled to the model resolution if necessary. AMCLIM was set up to use a one-year spin-up in order to keep an annual cycle of simulation period for each grid. Detailed descriptions of the global application of AMCLIM can be found in refs[23,24].

We use the percentage of N that is lost via NH_3 emissions, P_V, as an indicator of NH_3 volatilization, which is expressed as follows:

$$P_{\mathrm{V}} = \frac{F_{\mathrm{NH_3(annual\ total)}}}{N_{\mathrm{activity}}} \times 100 \qquad (4)$$

where N_{activity} refers to excreted flux of N in livestock houses for housing, stored or managed N from livestock excreta for manure management, excreted N on pastures by ruminants for grazing, applied N from manure and synthetic fertilizer for land application of manure and synthetic fertilizer, respectively. $F_{\mathrm{NH_3(annual\ total)}}$ is the annual total NH_3 emission from the

corresponding activity. The P_V was also used to derive a set of generalised EFs for synthetic fertilizer use and livestock systems from the baseline simulations. We calculated global average EFs (expressed in the same way as P_V) for synthetic fertilizer application (16% for urea and 13% for non-urea fertilizer such as ammonium nitrate), and for each type of livestock with all management stages included (see Supplementary Table 4). These global average EFs varied across each activity source were then used to generate a comparison map that show spatial differences between the baseline results and EF-derived emissions (Fig. 1b).

Temperature perturbation experiments were performed with temperatures (both air and ground) increased and decreased by 2 ºC, while other conditions were kept the same as the baseline simulations (the soil water content was not simulated explicitly in these experiments). The temperature sensitivity k_T at present state is derived from the relative change in P_V due to ±2 °C normalised by temperature change, using following equation:

$$k_{\mathrm{T}} = \frac{dP_{\mathrm{V}}}{P_{\mathrm{V}} dT_{\mathrm{air}}} \quad (5)$$

We examined a simple package of six linked mitigation measures for NH_3 emission abatement. By a “simple package” we mean: a) a short-list of measures that are widely available and cost-effective (as informed by the UNECE Ammonia Guidance Document[40]), b) a combined package that fits simply and logically together, where the selected measures complement each other, as outlined in Chapter 7 of the UNECE Guidance Document on Integrated Sustainable Nitrogen Management[39], and which c) draw on simple principles of Sustainable Nitrogen Management as outlined in Chapter 2 of the same UNECE nitrogen guidance document[39]. By cost-effective, we mean measures that with basic investment can typically pay for themselves considering fertilizer N and other benefits to farmers, for which see Sutton et al.[61] . The simulated package of six measures consisted of:

A1: decreasing application rates of synthetic N fertilizer by 20% (matching to N savings accomplished by measures A2, B2, C1 and C2, in accordance with UNECE Principle 6[39], that reductions in N losses should be matched by reductions in N inputs to avoid pollution swapping).

A2: incorporation, deep placement or injection of 25% of fertilizers and manure applied to field, which reduces exposure of these N resources to the atmosphere. We selected this modest ambition of 25% (rather than 100%) to emphasise that the approach be focused in the most cost-effective situations (e.g. largest farms or where sufficient labour available); a more ambitious strategies could assume a higher share.

B1: reducing livestock N excretion by 10% through improved animal feed. This operates on the UNECE principle[39], that reducing N inputs by improved diets (e.g. avoiding excess crude protein intake) leads to reduced excretion and hence reduced NH_3 emissions

B2: decreasing emitting surface area in houses by 20%. This measure applies the simple UNECE principle[39] that reducing the area of manure exposed to the atmosphere tends to reduce NH_3 emissions.

C1 and C2: covering storage tanks holding of liquid manure (C1) and properly storing solid manure in covered storage units (C2). This simple measures applies the same UNECE principle[39] as B2. Covering manure stores also avoids odour and helps retain valuable fertilizer value of manures.

As compared with the full list of 74 measures identified by the UNECE Nitrogen Guidance Document[39], this short list of six basic and widely cost-effective measures can thus be considered as a simple package. The selection is informed by comparison of cost-effectiveness, noting that some measures (not selected here), such as scrubbing of exhaust air of animal houses, tend to be more expensive[61]. Cost-effectiveness will vary regionally (e.g. in relation to

labour and capital costs and detailed mode of implementation), but the underlying principles are common to all regions.

We first quantify the effect of each measure on NH_3 abatement individually and then applied all six mitigation practices as a package to evaluate the integrated reduction. Details are given in Supplementary Note 4 and Supplementary Table 3.

Estimated NH_3 emissions under climate scenarios

We estimate future NH_3 emissions under four Shared Socioeconomic Pathways (SSPs): SSP1-2.6, SSP2-4.5, SSP3-7.0 and SSP5-8.5, respectively[62]. These pathways represent climate change scenarios for different levels of radiative forcing resulting from greenhouse gas emissions. We focus on investigating the effects of temperature changes on NH_3 emissions. We use near-surface air temperature from eight Earth Systems Models (ESMs) in the context of Coupled Model Intercomparison Project Phase 6 (CMIP6).

These ESMs include CanESM5, CESM2, CIESM, GFDL-ESM4, IPSL-CM6A-LR, MPI-ESM1-2-LR, MRI-ESM2-0 and UKESM1-0-LL, which together form a range of plausible climate projections. We applied AMCLIM to simulate global agricultural NH_3 emissions for the year 2010, which is then set as the baseline simulation to derive the baseline volatilization percentage, P_V. Subsequently, we performed four rounds of temperature perturbation experiments with near-surface air temperature (at 2 m) changed by -2, +2, +5 and +10 ºC. The P_V of these four groups of experiments were calculated, which were then used to perform linear interpolation. By doing this, we are able to find the relative changes in P_V due to temperature change. We projected annual mean volatilization rates using future temperature data provided by the ensemble mean of eight climate models under the four SSP scenarios (SSP1-2.6, SSP2-4.5, SSP3-7.0 and SSP5-8.5). Subsequently, the projected NH_3 emissions are calculated from the following equation:

$$F_{\mathrm{NH_3}} = \sum P_{\mathrm{V,activity}} F_{\mathrm{N,activity}} \quad (6)$$

where $F_{\mathrm{N,activity}}$ is the annual total N input from agricultural sectors, assuming the same activity data as the reference year 2010. Since it is difficult to determine the amount of N from manure storage and application to land (as this is related to previous stages), an aggregated temperature sensitivity is calculated for the overall volatilization from housing, manure storage/processing and land-application together.

Data availability

The ERA5 reanalysis data are available at https://www.ecmwf.int/en/forecasts/dataset/ecmwf-reanalysis-v5. The GGCMI3 N application rate and crop calendar data are available at https://zenodo.org/records/5176008#.YZPVhL3P3_Q. Livestock data from GLEAM2 are available upon request. Modelling results of the baseline simulations presented in this study are in netCDF format and can be freely accessed from the Edinburgh DataShare

(https://doi.org/10.7488/ds/7710, Jiang et al., 2024) and (https://doi.org/10.7488/ds/7888, Jiang et al., 2025). Modelled temperature sensitivity data and future projections are deposited at the Edinburgh DataShare (https://doi.org/10.7488/ds/8022, Jiang et al., 2025).

Code availability

Code of the AMCLIM model can be obtained from GitHub (https://github.com/jjzwilliam/AMCLIM, last access: 3 April 2024) and Zenodo (https://doi.org/10.5281/zenodo.10911886, Jiang, 2024).

Acknowledgements

This study was supported by the Global Environment Facility (GEF) through the UN Environment Programme (UNEP) for the project “Towards the International Nitrogen Management System (Towards INMS)”, the UKRI under its Global Challenges Research Fund for support of the GCRF South Asian Nitrogen Hub (grant no. NE/S009019/2), the NERC National Capability support, including through the CEH SUNRISE project and the ReCLEAN Joint Initiative at ETH Zurich under the ETH Board Joint Initiatives scheme. We thank the UK national supercomputing ARCHER2 and ETH Zurich high-performance cluster Euler.

Author information

Authors and affiliations

School of GeoSciences, The University of Edinburgh, Edinburgh, United Kingdom

Jize Jiang, David S. Stevenson

Department of Environmental Systems Science, ETH Zurich, Zurich, Switzerland

Jize Jiang

Eawag, Swiss Federal Institute of Aquatic Science and Technology, Dübendorf, Switzerland

Jize Jiang

Animal Production and Health Division, Food and Agriculture Organization of the United Nations, Rome, Italy

Aimable Uwizeye, Flavia Casu, Giuseppe Tempio, Alessandra Falcucci

UK Centre for Ecology and Hydrology, Edinburgh, United Kingdom

Mark A. Sutton

Contributions

J.J., D.S.S. and M.A.S. designed the research. J.J. developed the model, performed the simulations and analysed the data. A.U., F.C., G.T. and A.F. provided model input data. J.J. and M.A.S wrote the draft of paper. All authors contributed to interpretation of results and critical revision of the paper.

Corresponding author

Correspondence to Jize Jiang, David S. Stevenson and Mark A. Sutton

Competing interests

The authors declare no competing interests.

Reference

1. Galloway, J. N. et al. The Nitrogen Cascade. BioScience 53, 341 (2003).
2. Sutton, M. A. et al. Too much of a good thing. Nature 472, 159–161 (2011).
3. Anderson, N., Strader, R. & Davidson, C. Airborne reduced nitrogen: ammonia emissions from agriculture and other sources. Environ. Int. 29, 277–286 (2003).
4. Fowler, D. et al. Atmospheric composition change: Ecosystems–Atmosphere interactions. Atmos. Environ. 43, 5193–5267 (2009).
5. Nitrogen as a threat to European air quality. in The European Nitrogen Assessment 405–433 (Cambridge University Press, 2011). doi:10.1017/cbo9780511976988.021.
6. Bauer, S. E. et al. Nitrate aerosols today and in 2030: a global simulation including aerosols and tropospheric ozone. Atmospheric Chem. Phys. 7, 5043–5059 (2007).
7. Malm, W. C., Schichtel, B. A., Pitchford, M. L., Ashbaugh, L. L. & Eldred, R. A. Spatial and monthly trends in speciated fine particle concentration in the United States. J. Geophys. Res. Atmospheres 109, (2004).
8. Brunekreef, B. & Holgate, S. T. Air pollution and health. The Lancet 360, 1233–1242 (2002).
9. Pinder, R. W., Gilliland, A. B. & Dennis, R. L. Environmental impact of atmospheric NH_3 emissions under present and future conditions in the eastern United States. Geophys. Res. Lett. 35, (2008).
10. Krupa, S. V. Effects of atmospheric ammonia (NH_3) on terrestrial vegetation: a review. Environ. Pollut. 124, 179–221 (2003).
11. Sutton, M. A. et al. Alkaline air: changing perspectives on nitrogen and air pollution in an ammonia-rich world. Philos. Trans. R. Soc. Math. Phys. Eng. Sci. 378, 20190315 (2020).
12. Bouwman, A. F. et al. A global high-resolution emission inventory for ammonia. Glob. Biogeochem. Cycles 11, 561–587 (1997).

13. Behera, S. N., Sharma, M., Aneja, V. P. & Balasubramanian, R. Ammonia in the atmosphere: a review on emission sources, atmospheric chemistry and deposition on terrestrial bodies. Environ. Sci. Pollut. Res. 20, 8092–8131 (2013).
14. Sutton, M. A. et al. Towards a climate-dependent paradigm of ammonia emission and deposition. Philos. Trans. R. Soc. B Biol. Sci. 368, 20130166 (2013).
15. Riddick, S. N. et al. The global distribution of ammonia emissions from seabird colonies. Atmos. Environ. 55, 319–327 (2012).
16. Jiang, J., Stevenson, D. S., Uwizeye, A., Tempio, G. & Sutton, M. A. A climate-dependent global model of ammonia emissions from chicken farming. Biogeosciences 18, 135–158 (2021).
17. Sutton, M. A., Schjørring, J. K. & Wyers, G. P. Plant—atmosphere exchange of ammonia. Philos. Trans. R. Soc. Lond. Ser. Phys. Eng. Sci. 351, 261–278 (1995).
18. Nemitz, E., Milford, C. & Sutton, M. A. A two-layer canopy compensation point model for describing bi-directional biosphere-atmosphere exchange of ammonia. Q. J. R. Meteorol. Soc. 127, 815–833 (2001).
19. Flechard, C. R. et al. Advances in understanding, models and parameterizations of biosphere-atmosphere ammonia exchange. Biogeosciences 10, 5183–5225 (2013).
20. Móring, A. et al. A process-based model for ammonia emission from urine patches, GAG (Generation of Ammonia from Grazing): description and sensitivity analysis. Biogeosciences 13, 1837–1861 (2016).
21. Bash, J. O., Cooter, E. J., Dennis, R. L., Walker, J. T. & Pleim, J. E. Evaluation of a regional air-quality model with bidirectional NH_3 exchange coupled to an agroecosystem model. Biogeosciences 10, 1635–1645 (2013).
22. Fu, X. et al. Estimating NH_3 emissions from agricultural fertilizer application in China using the bi-directional CMAQ model coupled to an agro-ecosystem model. Atmospheric Chem. Phys. 15, 6637–6649 (2015).

23. Jiang, J., Stevenson, D. S. & Sutton, M. A. A dynamical process-based model for quantifying global agricultural ammonia emissions – AMmonia–CLIMate v1.0 (AMCLIM v1.0) – Part 1: Land module for simulating emissions from synthetic fertilizer use. Geosci. Model Dev. 17, 8181–8222 (2024).
24. Jiang, J. et al. A dynamical process-based model for quantifying global agricultural ammonia emissions – AMmonia–CLIMate v1.0 (AMCLIM v1.0) – Part 2: livestock farming. Geosci. Model Dev. 18, 5051–5099 (2025).
25. Xu, R. T. et al. Half-Century Ammonia Emissions From Agricultural Systems in Southern Asia: Magnitude, Spatiotemporal Patterns, and Implications for Human Health. GeoHealth 2, 40–53 (2018).
26. Xu, R. et al. Global ammonia emissions from synthetic nitrogen fertilizer applications in agricultural systems: Empirical and process-based estimates and uncertainty. Glob. Change Biol. 25, 314–326 (2019).
27. Vira, J., Hess, P., Melkonian, J. & Wieder, W. R. An improved mechanistic model for ammonia volatilization in Earth system models: Flow of Agricultural Nitrogen version 2 (FANv2). Geosci. Model Dev. 13, 4459–4490 (2020).
28. Beaudor, M. et al. Global agricultural ammonia emissions simulated with the ORCHIDEE land surface model. Geosci. Model Dev. 16, 1053–1081 (2023).
29. Beaudor, M., Vuichard, N., Lathière, J. & Hauglustaine, D. Future trends of global agricultural emissions of ammonia in a changing climate. J. Adv. Model. Earth Syst. 17, 1–18 (2025).
30. Beusen, A. H. W., Bouwman, A. F., Heuberger, P. S. C., Van Drecht, G. & Van Der Hoek, K. W. Bottom-up uncertainty estimates of global ammonia emissions from global agricultural production systems. Atmos. Environ. 42, 6067–6077 (2008).
31. Yang, Y. et al. Improved global agricultural crop- and animal-specific ammonia emissions during 1961–2018. Agric. Ecosyst. Environ. 344, 108289 (2023).

32. Paulot, F. et al. Ammonia emissions in the United States, European Union, and China derived by high-resolution inversion of ammonium wet deposition data: Interpretation with a new agricultural emissions inventory (MASAGE_NH3). J. Geophys. Res. Atmospheres 119, 4343–4364 (2014).
33. Crippa, M. et al. Gridded emissions of air pollutants for the period 1970–2012 within EDGAR v4.3.2. Earth Syst. Sci. Data 10, 1987–2013 (2018).
34. Tian, H. et al. History of anthropogenic Nitrogen inputs (HaNi) to the terrestrial biosphere: a 5 arcmin resolution annual dataset from 1860 to 2019. Earth Syst. Sci. Data 14, 4551–4568 (2022).
35. Xu, P. et al. Fertilizer management for global ammonia emission reduction. Nature 626, 792–798 (2024).
36. Skjøth, C. A. & Geels, C. The effect of climate and climate change on ammonia emissions in Europe. Atmospheric Chem. Phys. 13, 117–128 (2013).
37. Shen, H. et al. Intense Warming Will Significantly Increase Cropland Ammonia Volatilization Threatening Food Security and Ecosystem Health. One Earth 3, 126–134 (2020).
38. Xu, X. et al. Climate change may interact with nitrogen fertilizer management leading to different ammonia loss in China's croplands. Glob. Change Biol. 27, 6525–6535 (2021).
39. Sutton, M. A., Howard, C. M., Mason, K. E., Brownlie, W. J. & Cordovil, C. M. d. S. Nitrogen Opportunities for Agriculture, Food & Environment: UNECE Guidance Document on Integrated Sustainable Nitrogen Management. (UK Centre for Ecology & Hydrology, Wallingford, 2022).
40. Bittman, S., Dedina, M., Howard, C. M. (Clare), Oenema, O. & Sutton, M. A. Options for Ammonia Mitigation: Guidance from the UNECE Task Force on Reactive Nitrogen. (Centre for Ecology & Hydrology, on behalf of Task Force on Reactive Nitrogen, of the UNECE Convention on Long Range transboundary Air Pollution, Edinburgh, 2014).

41. Lin, Z. et al. Effects of Nitrogen Application Levels on Ammonia Volatilization and Nitrogen Utilization during Rice Growing Season. Rice Sci. 19, 125–134 (2012).
42. Chen, A. et al. Characteristics of ammonia volatilization on rice grown under different nitrogen application rates and its quantitative predictions in Erhai Lake Watershed, China. Nutr. Cycl. Agroecosystems 101, 139–152 (2015).
43. Liu, T. Q. et al. Deep placement of nitrogen fertilizers reduces ammonia volatilization and increases nitrogen utilization efficiency in no-tillage paddy fields in central China. Field Crops Res. 184, 80–90 (2015).
44. Yao, Y. et al. Urea deep placement for minimizing NH3 loss in an intensive rice cropping system. Field Crops Res. 218, 254–266 (2018).
45. Uwizeye, A. et al. Nitrogen emissions along global livestock supply chains. Nat. Food 1, 437–446 (2020).
46. Van Dijk, M., Morley, T., Rau, M. L. & Saghai, Y. A meta-analysis of projected global food demand and population at risk of hunger for the period 2010–2050. Nat. Food 2, 494–501 (2021).
47. Summary for Policymakers. in Climate Change 2021 – The Physical Science Basis 3–32 (Cambridge University Press, 2023). doi:10.1017/9781009157896.001.
48. Siman, F. C., Andrade, F. V. & Passos, R. R. Nitrogen Fertilizers and NH_3 Volatilization: Effect of Temperature and Soil Moisture. Commun. Soil Sci. Plant Anal. 51, 1283–1292 (2020).
49. Dong, W., Xing, H., Chen, S. & Hu, C. NH_3 emission responses to irrigation time and the initial moisture from urea applied to three soils in the North China Plain*. Irrig. Drain. 70, 1368–1380 (2021).
50. Frößl, J., Scholl, M., Hartung, J., Ruser, R. & Müller, T. How do soil moisture and simulated rainfall drive ammonia emissions after applying inhibited urea fertilizers? – An incubation study. J. Environ. Manage. 376, 124435 (2025).

51. Kanter, D. R. et al. A framework for nitrogen futures in the shared socioeconomic pathways. Glob. Environ. Change 61, 102029 (2020).
52. Sutton, M. A. et al. The nitrogen decade: mobilizing global action on nitrogen to 2030 and beyond. One Earth 4, 10–14 (2021).
53. Gu, B. et al. Abating ammonia is more cost-effective than nitrogen oxides for mitigating $PM_{2.5}$ air pollution. Science 374, 758–762 (2021).
54. Sutton, M. A., Burkhardt, J. K., Guerin, D., Nemitz, E. & Fowler, D. Development of resistance models to describe measurements of bi-directional ammonia surface–atmosphere exchange. Atmos. Environ. 32, 473–480 (1998).
55. Hersbach, H. et al. The ERA5 global reanalysis. Q. J. R. Meteorol. Soc. 146, 1999–2049 (2020).
56. Wieder, W. R., Boehnert, J. & Bonan, G. B. Evaluating soil biogeochemistry parameterizations in Earth system models with observations. Glob. Biogeochem. Cycles 28, 211–222 (2014).
57. Robinson, T. P. et al. Mapping the Global Distribution of Livestock. PLoS ONE 9, e96084 (2014).
58. Hurtt, G. C. et al. Harmonization of global land use change and management for the period 850–2100 (LUH2) for CMIP6. Geosci. Model Dev. 13, 5425–5464 (2020).
59. Mueller, N. D. et al. Closing yield gaps through nutrient and water management. Nature 490, 254–257 (2012).
60. Monfreda, C., Ramankutty, N. & Foley, J. A. Farming the planet: 2. Geographic distribution of crop areas, yields, physiological types, and net primary production in the year 2000. Glob. Biogeochem. Cycles 22, (2008).
61. Sutton, M. A. et al. Ammonia mitigation for economic and environmental benefits. (2025).
62. Van Vuuren, D. P. et al. The Shared Socio-economic Pathways: Trajectories for human development and global environmental change. Glob. Environ. Change 42, 148–152 (2017).

Figure captions

Fig. 1. Global annual agricultural NH_3 emissions. (a) Geographical distributions of NH_3 emissions calculated from the full AMCLIM application, taking account of climate and management differences (base run for 2010, excluding mitigation measures). White areas indicate that the activity data and hence NH_3 emissions are zero. (b) Comparison between NH_3 emissions calculated from the full AMCLIM application and emissions using an Emission Factor (EF) approach for each sector combined with sector activity statistics. The values are the ratio of NH_3 emissions using the full AMCLIM application divided by EF-based emissions.

Fig. 2. Temperature sensitivity of NH_3 volatilization. Temperature sensitivity is expressed as percentage change in the fraction of available N volatilized as NH_3 per °C compared with baseline emissions for 2010 (excluding mitigation measures). (a) All crop and livestock sources (b) synthetic fertilizer use, (c) livestock housing (d) manure storage (inc. manure processing) (e) manure application to land and (f) grazing.

Fig. 3. Geographical distribution of projected changes in agricultural NH_3 emissions. Comparisons between baseline estimates for 2010 and projections for 2091-2100 under four SSP scenarios (a) SSP1-2.6 (b) SSP2-4.5 (c) SSP3-7.0 and (d) SSP5-8.5. The focus here is on the temperature effects of these SSP scenarios; other socio-economic effects (e.g. on fertilizer use, livestock numbers) are intentionally excluded. The simulations are shown for runs without inclusion of emission mitigation measures.

Fig. 4. Projected NH_3 emissions in 2100 under four future climate scenarios and emission reductions estimated to be achieved applying a package of six agricultural management measures. (a) Global and regional increases in NH_3 emissions under the four SSP scenarios compared with 2010 (assuming the same activity level and considering climate effects only). (b) Effectiveness (dimensionless) of future NH_3 emissions mitigation under climate warming, being the ratio of emission reduction for each future scenario relative to the reduction achieved for 2010 (see Table 2), for a package of six mitigation measures applied equally in all the climate scenarios. A negative value of effectiveness means that the increase in emissions due to warming exceeds mitigation. The SSP climate scenarios are based on the Shared Socioeconomic Pathways approach, with radiative forcing increasing by 2.6 (least warming), 4.5, 7.0 or 8.5 W m^{-2} (greatest warming), denoted as SSP1–2.6, SSP2-4.5, SSP3-7.0 and SSP5–8.5, respectively. As with Fig. 3, the focus is on climate warming interactions, and the effects of other socio-economic drivers are deliberately excluded. The boxplots show the mean (black dots), median (horizontal lines), 25th to 75th percentile (boxes) and 5th to 95th percentile (whiskers) of the estimated changes for global and regional emissions from 2091-2100 relative to the baseline year 2010. The region boundaries are shown in Supplementary Fig. 10.

Editorial summary:

Global warming substantially weakens the effectiveness of agricultural ammonia-reduction measures, creating a significant climate penalty that demands integrated climate and air-quality policies, based on a process-based emission model.

Peer review information:

Communications Earth and Environment thanks Peng Xu and the other, anonymous, reviewer(s) for their contribution to the peer review of this work. Primary Handling Editors: Jinfeng Chang and Mengjie Wang. A peer review file is available

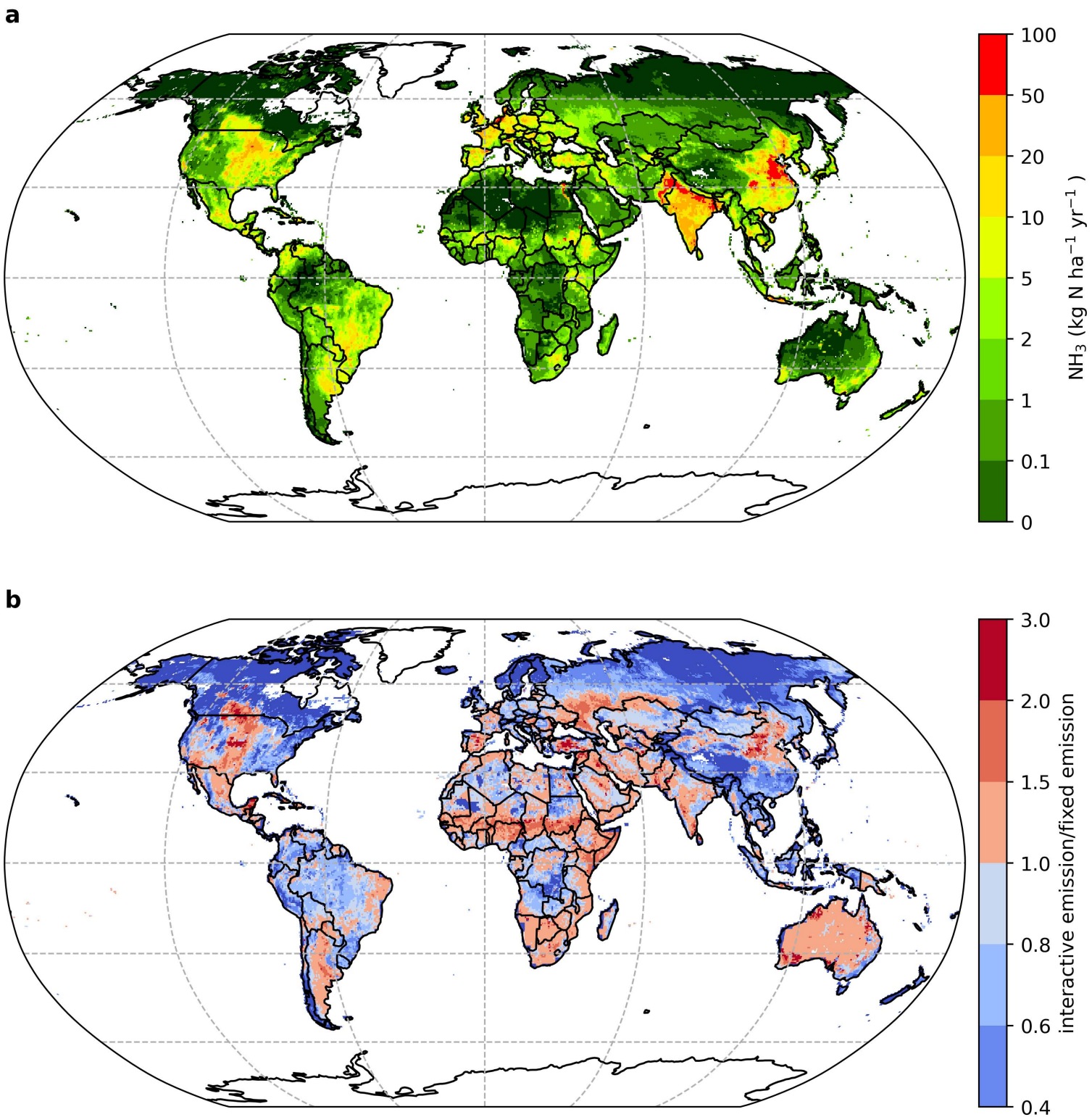
a
100
50
20
10
5
2
1
0.1
0
NH3 (kg N ha−1 yr−1)
b
3.0
2.0
1.5
1.0
0.8
0.6
0.4
interactive emission/fixed emission

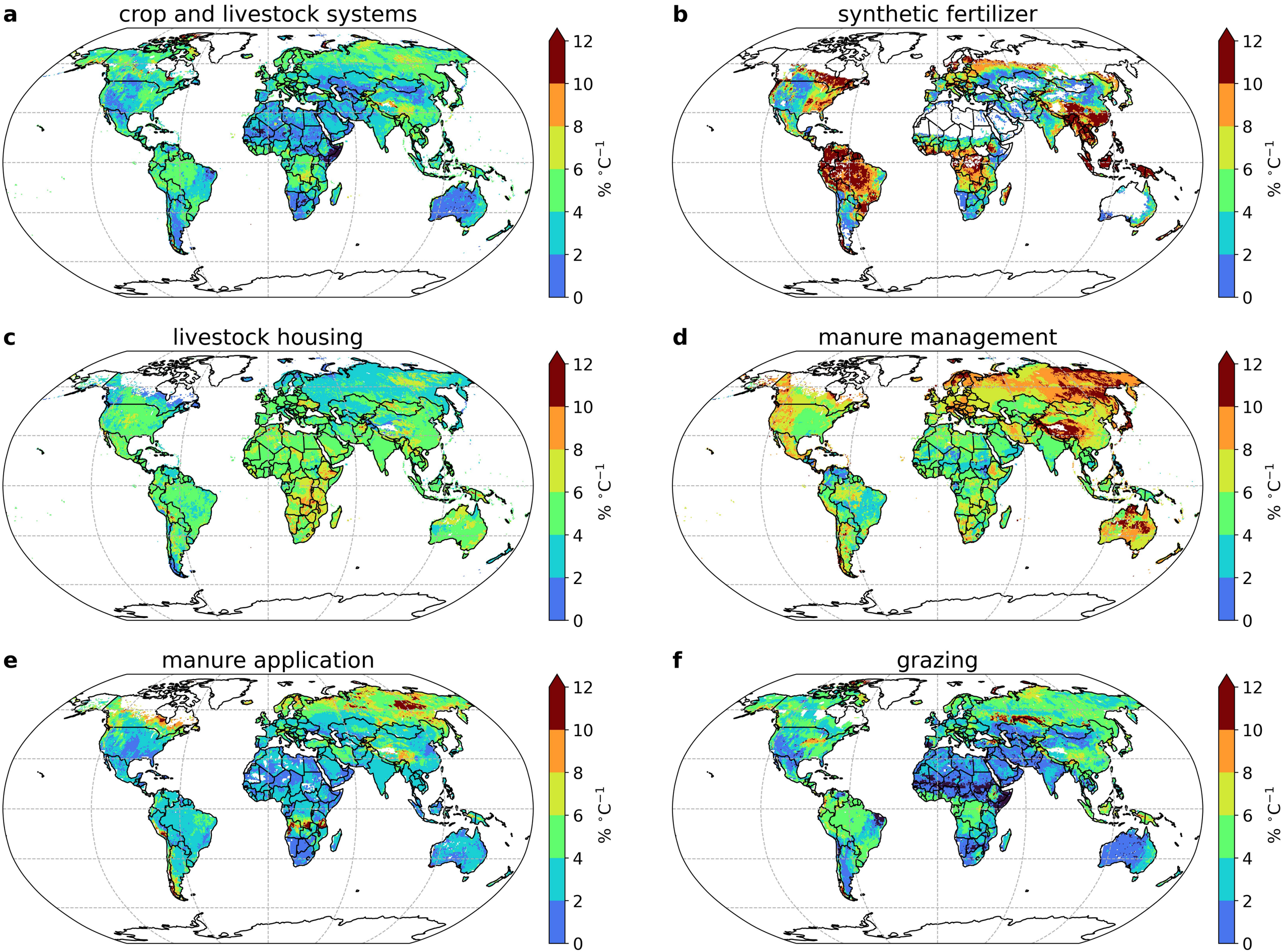
a
crop and livestock systems
b
synthetic fertilizer
c
livestock housing
d
manure management
e
manure application
f
grazing
0
2
4
6
8
10
12
% °C⁻¹

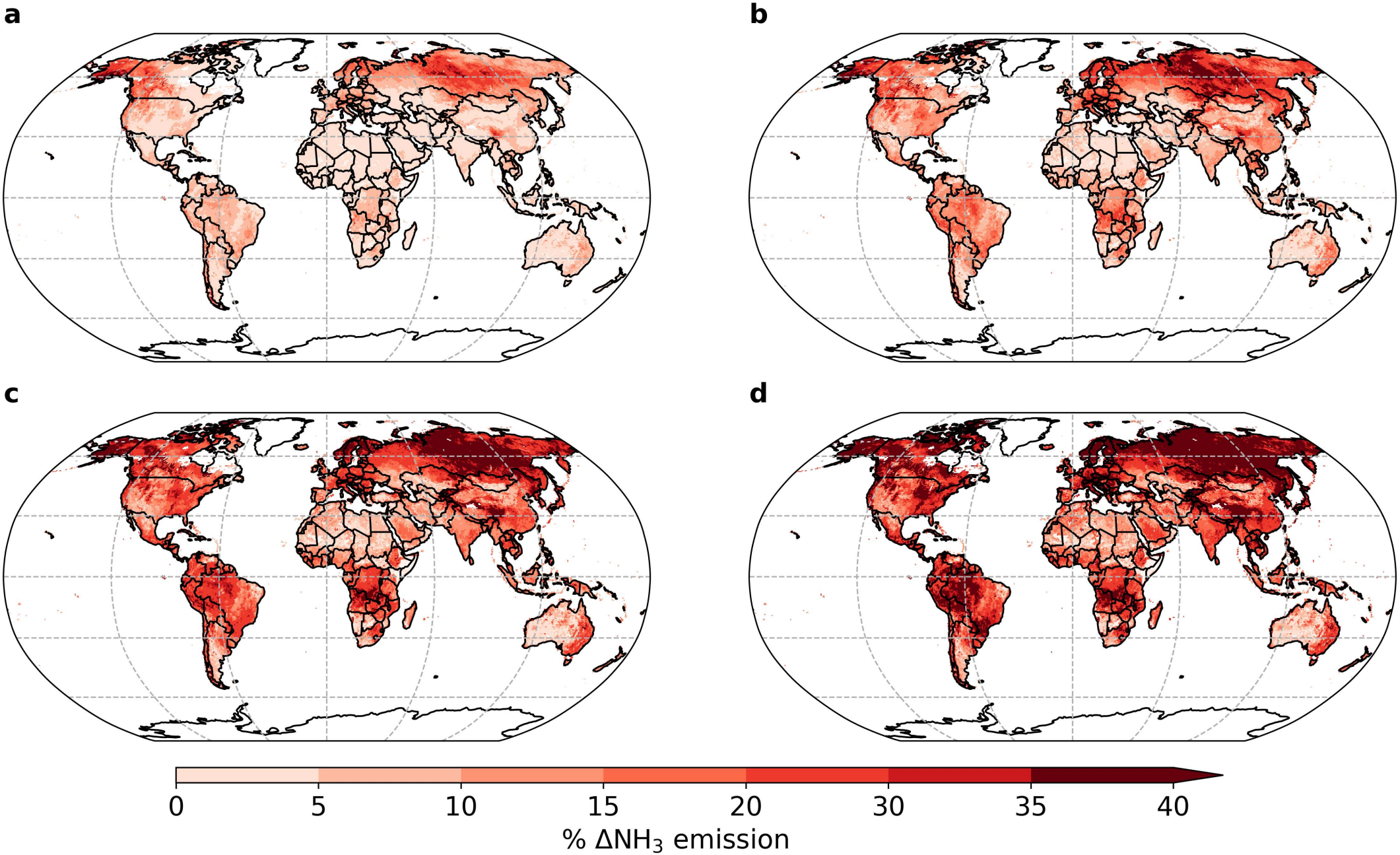
a
b
c
d
0
5
10
15
20
30
35
40
% ΔNH3 emission

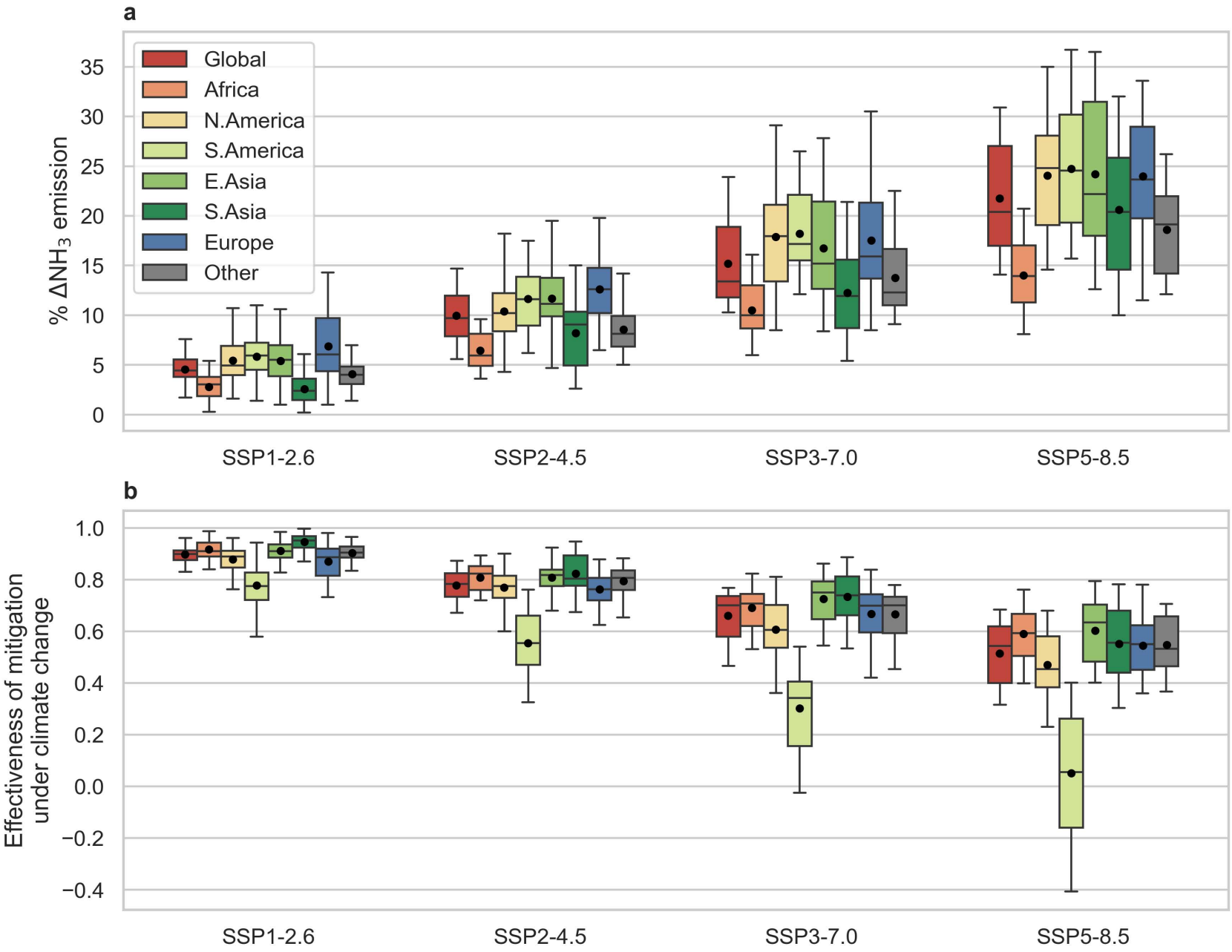
a
Global
Africa
N.America
S.America
E.Asia
S.Asia
Europe
Other
% ΔNH3 emission
35
30
25
20
15
10
5
0
SSP1-2.6
SSP2-4.5
SSP3-7.0
SSP5-8.5
b
Effectiveness of mitigation under climate change
1.0
0.8
0.6
0.4
0.2
0.0
−0.2
−0.4
SSP1-2.6
SSP2-4.5
SSP3-7.0
SSP5-8.5